Journal of Oceanology and Limnology
Vol. 40 No. 4, P. 1615-1627, 2022
https://doi.org/10.1007/s00343-021-1125-7

Reduced salinity interacts with ultraviolet radiation to alter photosystem II function in diatom *Skeletonema costatum**

Shasha ZANG[1, #], Fang YAN[1, #], Daode YU[2], Jingjing SONG[2], Lei WANG[1, 3], Zhiguang XU[1, 3, **], Hongyan WU[1, 3, **]

[1] *College of Life Science, Ludong University, Yantai 264025, China*

[2] *Marine Science Research Institute of Shandong Province, Qingdao 266104, China*

[3] *Key Laboratory of Marine Biotechnology in Universities of Shandong (Ludong University), Yantai 264025, China*

Received Apr. 14, 2021; accepted in principle May 31, 2021; accepted for publication Aug. 25, 2021

Abstract To investigate the effect of reduced salinity on diatoms' capacity to cope with changing ultraviolet radiation (UVR) and photosynthetically active radiation (PAR), *Skeletonema costatum* was grown in a range of salinity (15, 25, and 35). The photosystem II (PSII) function was analyzed by increasing PAR and UVR to mimic a mixing event in turbulent waters. The results show that high UVR exposure significantly reduced PSII activity, especially in cells grown at low salinity. UVR, but not salinity, stimulated the 'removal' rate of PSII protein PsbA. Salinity alone, in the range of 15 to 35, did not regulate PSII acceptor region; however, the low salinity+UVR treatment decreased the energy flux for electron transport per PSII reaction center in *S. costatum*. It showed that low salinity exacerbated the damaging effect of UVR on PSII function in *S. costatum* by suppressing PsbA protein synthesis and modifying the photochemistry of PSII. Although higher catalase (CAT) activity and NPQs were induced, they were unable to prevent the combined damage effect of low salinity+UVR. Our findings indicate that reduced salinity and increased UVR potentially affect the abundance and distribution of *S. costatum* with the escalation of climate disturbances.

Keyword: diatom; ultraviolet radiation (UVR); photoinactivation; photosystem II

1 INTRODUCTION

Diatoms (Bacillariophyceae) are essential microalgae that make up a major portion of the phytoplankton population and, as such, account for ~20% of the global primary productivity (Falkowski, 2012; Young and Morel, 2015). They are most often found in turbulent coastal waters where rapid vertical mixing leads to vastly irregular light exposure (MacIntyre et al., 2000). Exposure to a sudden bright light can produce oxidative stress which destroys the photosynthetic apparatus (Nishiyama et al., 2006; Nishiyama and Murata, 2014), leading to net photoinactivation. To protect this system, diatoms oppose PSII photoinactivation via proteolysis of photodamaged proteins from the thylakoid membrane (Silva et al., 2003; Nixon et al., 2010) prior to reinsertion with newly formed protein (Nixon et al., 2010; Komenda et al., 2012; Barnett et al., 2015). Another important strategy of diatoms to cope with excitation of photosystems is to activate the non-photochemical quenching (NPQ), which, in turn, triggers the trans-thylakoid proton gradient and activates the xanthophyll cycle (Lavaud and Lepetit, 2013; Lavaud and Goss, 2014). In addition, excessive light exposure induced the formation of reactive oxygen species (ROS) viz. superoxide anion (O_2^-) and peroxides. Superoxide dismutase (SOD) is the first enzyme of the enzymatic antioxidative pathway to convert superoxide radical into H_2O_2, which is subsequently neutralized to H_2O catalase (CAT).

* Supported by the Shandong Provincial Natural Science Foundation (Nos. ZR2019MC015, ZR2020QC025, ZR2020MD092), the open project of Rongcheng Marine Industrial Technology Research Institute, Ludong University (No. KF20180001), and the Key Technology Research and Development Program of Shandong (No. 2019GSF107091)
** Corresponding authors: bigwide@163.com; sdwuhongyan@126.com
# Shasha ZANG and Fang YAN contributed equally to this work and should be regarded as co-first authors.

These antioxidant enzymes not only control the steady state level of the reactive oxygen species but also allow them to perform important functions at specific sites under a variety of environmental conditions. The global mean atmospheric temperature is projected to rise up to 6 °C by the year 2100 (Intergovernmental Panel on Climate Change, 2013; Gattuso et al., 2015). A rise in temperature may increase the moisture-holding capacity of the atmosphere (Trenberth and Jones, 2007), enhance freshwater run-off into coastal zones (Rückamp et al., 2011; Pawlowicz, 2015), and intensify seasonal ice melt (Screen and Simmonds, 2010; Bintanja et al., 2013; Thorpe and Andrews, 2014). This would, subsequently, lead to reduced salinity, particularly in regions of mid/high latitudes (Intergovernmental Panel on Climate Change, 2013). Evidently, a steep decrease in salinity was reported in the Norwegian Sea coastline since the early 1970s, and worse yet, some regions exceeded 0.5 practical salinity units (Blindheim et al., 2000). A reduction in the average coastal salinity by approximately 5 was reported in the western coastal area of Greenland (Kamenos et al., 2012), and in China, large variations in salinity in the coastal waters of Jiangsu province due to freshwater inputs from high rain fall was reported (Kang et al., 2016; Gao et al., 2019). Salinity fluctuations could cause osmotic stress and change the cellular ionic composition of *Synechococcus* sp. (Allakhverdiev et al., 2000); therefore affecting a wide variety of metabolic pathways (Balzano et al., 2011; Kirrolia et al., 2011). For instance, growth rate, photosynthetic activity, and carbon fixation rate in the diatom *Thalassiosira weissflogii* was shown to be reduced with a decrease in salinity from 35 to 15 (Radchenko and Il'yash, 2006). The opposite phenomenon was observed in *Emiliania huxleyi*, with growth rate, cell size, and photosynthetic performance increasing with the reduction in salinity from 35 to 25 (Xu et al., 2020). In addition, there are species that show a strong capacity to adapt to a large fluctuation in salinity levels: for example, the optimal growth of *Tetraselmis suecica* remained constant in salinity from 20 to 60, however, both growth and photosynthetic activity were inhibited at a salinity of 10 (Pugkaew et al., 2019).

Due to climate change and stratospheric ozone depletion, the level of solar ultraviolet radiation (UVR) exposure has increased dramatically (Bais et al., 2019). Efforts have been made to assess the harmful consequence of UVR on the phytoplankton population (Häder et al., 2015; Williamson et al., 2019). UVR was shown to damage DNA and protein molecules, suppress utilization of carbon, nitrogen, and other nutrients, stimulate ROS generation, and cause cell death (Häder et al., 2007, 2015). The growth and photosynthesis of phytoplankton are inhibited by UVR, and thus, the primary productivity is reduced (Harrison and Smith, 2009; Häder and Gao, 2017; Neale and Thomas, 2017). Alongside studies on the sole effects of salinity or UVR on marine microalgae, their synergistic effects have also been reported. Rijstenbil (2005) demonstrated that exposure to UVR alone elevated ROS generation and a combined exposure of UVR and high salinity (60) further increased ROS production by ~50% in *Cylindrotheca Closterium*. Similarly, Wu et al. (2017) reported that UVR and high salinity cooperatively decreased the photochemical activities of PSII in the benthic diatom *Nitzschia* sp. However, the effects of low salinity and UVR on the physiological activities of diatoms remain unclear and further studies need to be performed to identify the pathway(s) involved in the synergistic effect of UVR and low salinity on PSII function.

The diatom *Skeletonema costatum* is one of the most abundant harmful algal bloom causing organisms, found in coastal waters globally (Kooistra et al., 2008; Balzano et al., 2011; Boller et al., 2015). *S. costatum* has a wide salinity tolerance: it can sustain its growth well in salinities between 10 and 35 (Balzano et al., 2011), with maximum growth rate reported at salinities between 18 and 35, depending on growth conditions like temperature or irradiances (Yan et al., 2002; Rai and Rajashekhar, 2014). Because *S. costatum* are prevalent in turbulent waters, they experience frequent fluctuations in UVR and photosynthetically active radiation (PAR) levels. In this study, *S. costatum* was cultured under three salinity conditions (15, 25, and 35) and alterations in PsbA, photoinactivation, NPQs, CAT, and SOD activity, in response to PAR and PAR+UVR exposure, were examined. Our purpose was to examine how coastal salinity fluctuations regulate the ability of diatoms to adapt to fluctuating light.

2 MATERIAL AND METHOD

2.1 Strains and growth circumstances

Skeletonema costatum (Greville) Cleve (strain 2042) was obtained from the Institute of Oceanography, Chinese Academy of Sciences. For culture medium, natural seawater with a salinity of 35 obtained from

the coastal water was filter-sterilized through a 0.22-μm polycarbonate membrane filter (Corning, NY, USA) and enriched with f/2 medium solutions (Guillard and Ryther, 1962; Vartanian et al., 2009). The medium with a salinity of 35 was considered as a control for comparison of salinity-induced effects. The low and medium salinity seawater (15 and 25) was obtained by diluting the filtered seawater with distilled water and was amended with f/2 nutrients to the same levels as the control. Salinity was checked using a salinity meter (LS10T, Guangzhou, China).

Skeletonema costatum cultures were grown under 100-μmol/(m^2·s) PAR using white cool tubes of fluorescent with a 12-h:12-h light:dark cycle at 18 °C. The *S. costatum* underwent ~7 transfers of semi-continuous dilution to ensure uniform growth. The specific growth rates of *S. costatum* grown at 15, 25, and 35 were 0.25±0.02, 0.48±0.03, and 0.53±0.02 per day, respectively. Cells with steady growth rates were harvested for the following upward light exposure experiment. Each treatment was repeated four times.

2.2 Upward light shift and recovery assessment

Skeletonema costatum culture replicates with different salinity level were split into two UV-transparent quartz tubes, with 50-μg/mL lincomycin added to one quartz tube to block chloroplast protein synthesis (Bachmann et al., 2004; Gao et al., 2018), thereby inhibiting PSII repair (Tyystjärvi and Aro, 1996). Next, the tubes with and without lincomycin were placed in darkness for 10 min to allow the lincomycin to exert its effect and then exposed to simulated solar radiation at UVR 140 W/m^2 and PAR 26 W/m^2, which were set based on the averaged daytime solar irradiances for UVR and PAR measured locally in May when *S. costatum* red tide bursts out with high frequency. Two radiation treatments were applied: 1) cultures receiving PAR+UVR (295–700 nm): quartz tubes covered with Ultraphan film 295 (UV Opak, Digefra, Munich, Germany); 2) cultures receiving only PAR (400–700 nm): quartz tubes covered with Ultraphan film 395 (UV Opak, Digefra, Munich, Germany). The *S. costatum* cultures were maintained in a water bath at 18±1 °C.

The cultures received the solar radiation treatment for 120 min. Samples were collected at times 0 (before the onset of treatment), 15, 30, 60, 90, and 120 min after the onset of treatment and to measure chlorophyll fluorescence and protein analyses. After high light exposure, the *S. costatum* cultures were placed back under growth light (100-μmol/(m^2·s) PAR) for half hour to allow to recuperate. Samples were collected for the final analyses.

A solar simulator (Sol 1200, Dr. Hönle GmbH, Germany) equipped with a 1 000-W xenon arc lamp was used for the experiment. The output irradiance of UVR and PAR were measured with a broadband filter radiometer (ELDONET; Real Time Computer, Germany).

2.3 Chlorophyll fluorescence measurement and parameterization

To determine chlorophyll fluorescence parameters, a portable pulse amplitude modulated fluorometer (WATER-PAM, Walz, Germany) was used. The variable to maximal chlorophyll-*a* fluorescence ratio (F_v/F_m) of dark-adapted samples was used to represent the photochemical efficiency of PSII. The F_v/F_m ratio was calculated utilizing the minimal (F_0) and maximal (F_m) fluorescence yield of 5-min dark-adapted cells and calculated as: $F_v=(F_m-F_0)$. For measuring F_0 and F_m, the measuring and pulse of saturating light were maintained at <0.1 μmol/(m^2·s) and 4 000 μmol/(m^2·s), respectively.

The rate constant for photoinactivation (K_{pi}, /s), and the rate constant for PSII repair (K_{rec}, /s) were evaluated. K_{pi} was obtained from lincomycin-treated specimens via plotting a single-phase exponential decay through a plot of F_v/F_m versus the cumulative photons implemented during the bright light processing. K_{rec} was obtained from non-lincomycin-treated samples. Both measurements were performed conforming to the Kok equation (Kok, 1956; Campbell and Tyystjärvi, 2012):

$$\frac{Y_t}{Y_0}=\frac{K_{rec}}{K_{pi}+K_{rec}}+\frac{K_{pi}}{K_{pi}+K_{rec}}e^{-(K_{pi}+K_{rec})t}, \quad (1)$$

where Y_t and Y_0 illustrate the maximal quantum yield at time t and zero (seconds), respectively.

A sustained phase of NPQ (NPQs), which reflects an inducible elevation in the relaxation time for a fraction of NPQ, persisting beyond a 5-min dark period (Wu et al., 2012), was defined as:

$NPQs=(F_{mt0}-F_m)/F_m$.

where F_{mt0} and F_m are the values of F_m from dark-adapted cells taken at time zero (T_0) prior to the bright light processing, and at the reported time intervals, respectively.

2.4 Polyphasic rise of Chl-*a* fluorescence transients and the JIP-test

After 120-min high light exposure, 5-mL samples were collected from each independent culture (n=4).

The polyphasic nature of fluorescence transients due to Chl *a* was analyzed using a plant efficiency analyzer (Hansatech Instruments Ltd., UK). To begin, the samples were placed in absolute darkness for 5 min. The fluorescence signals were recorded within a time scan from 10 μs to 2 s, and labeled as steps O, J, I, and P. The JIP-test identified the energy flux in the membranes of the photosynthetic apparatus (Strasser et al., 2000). According to the energy flux model in JIP-test, photons are absorbed by the antennae pigments (ABS, absorption flux) which are excited. A part of this excitation energy, the trapping flux (TR), is transferred to the reaction center (RC) while the remaining part is dissipated either as fluorescence or as heat. In the RCs, the TR is converted to redox energy by reducing Q_A to Q_A^-, which is then reoxidized to Q_A, thus leading to an electron transport flux (ET) and consequently to photochemistry. The relative variable fluorescence at phases J (V_J), and the initial slope at the beginning of the variable fluorescence transients (theoretically at time zero) (M_0), the possibility of the electron transport beyond Q_A (ψ_0), and the energy fluxes for ABS, dissipation (DI), TR and ET per PSII reaction center can be shown in the following equations based on Strasser et al. (2000):

$$V_J=(F_{2ms}-F_0)/(F_m-F_0), \quad (2)$$

$$M_0=4\times(F_{300\mu s}-F_0)/(F_m-F_0), \quad (3)$$

$$\psi_0=1-V_J, \quad (4)$$

$$ABS/RC=M_0\times(1/V_J)\times[F_m/(F_m-F_0)], \quad (5)$$

$$TR_0/RC=M_0\times(1/V_J), \quad (6)$$

$$ET_0/RC=M_0\times(1/V_J)\times\psi_0, \quad (7)$$

$$DI_0/RC=(ABS/RC)-(TR_0/RC). \quad (8)$$

2.5 Quantitative immunoblotting

Culture samples (20 mL) were vacuum-filtered onto glass fiber filters (25-mm diameter, Whatman), and instantly flash frozen in liquid nitrogen before storing at -80 °C until further analysis. The whole available protein was measured utilizing a Lowry protein assay kit (Bio-Rad DC assay) followed by western blots for PSII PsbA subunit. Standard curve generation: total protein (2 μg per lane) was run alongside a range of known controls (15.625-, 31.25-, 62.5-, and 125-fmol PsbA) per lane (AS01 016S; Agrisera, www.agrisera.se). The PsbA protein levels were quantified against the standard curves of protein (Brown et al., 2008; Wu et al., 2011).

The PsbA protein clearance rate constant (K_{PsbA}, /s) was determined through plotting fmol PsbA per μg total protein for cells exposed to bright light and lincomycin exposure. The PsbA plot was then compared against a single-phase exponential decay under bright light exposure graph (Wu et al., 2012) to reveal the PsbA protein clearance rate from the PSII pool.

2.6 Measurement of CAT and SOD activity

After 120-min high light exposure, 20-mL samples were collected onto a membrane of polycarbonate (0.22 μm, Whatman) and washed with pH 7.6 phosphate buffer. The enzyme was extracted in 0.6-mL phosphate buffer (pH 7.6) containing 1-mmol/L ethylenediaminetetraacetic acid (EDTA), 50-mmol/L KH_2PO_4, and 1% (w/v) polyvinylpolypyrrolidone. Centrifuge the homogenized extract at 12 000×*g* at 4 °C for 10 min. CAT and SOD assessment kits (Nanjing Jiancheng Biological Engineering Company, China) were used to detect CAT activity and SOD, in accordance to manufacturer's protocols. One SOD activity unit equals to the enzyme quantity that promotes a 50% reduction in the nitro-blue tetrazolium depletion rate at 560 nm (Wang and Wang, 2010). CAT activity, on the other hand, was calculated by analyzing the initial disappearance rate of H_2O_2 at 240 nm (Li et al., 2015).

2.7 Statistical analysis

The outcomes are shown as means of replicates±standard error. The statistics data were derived utilizing SPSS v.22. The outcomes conformed to a normal distribution (Shapiro-Wilk, $P>0.05$) and the variances were considered equal (Levene's test, $P>0.05$). Two-way multivariate ANOVAs (MANOVAs) was employed to study the consequences of salinity, UVR and lincomycin on F_v/F_m, NPQs, PsbA content, CAT activity, and SOD activity in *S. costatum* at various durations of light exposure. Post hoc measurements were determined using a Tukey HSD. ANOVAs (RM-ANOVAs) were repeatedly measured to determine the influence of light exposure duration on PsbA content, F_v/F_m, and NPQs. The corresponding post hoc measurements were determined using a Tukey HSD. One-way ANOVAs analyzed the mean differences in parameters obtained from the JIP test, photoinactivation rate, PsbA removal rate, and PSII repair rate constant. $P<0.05$ is defined statistically significant.

Table 1 Repeated analysis of variance examining the consequence of light duration on F_v/F_m, PsbA, and NPQs in multiple environments

Item	F_v/F_m			PsbA			NPQs		
	df	*F*	Sig.	df	*F*	Sig.	df	*F*	Sig.
Time	5	4 311.293	<0.001	5	185.110	<0.001	5	549.461	<0.001
Time×salinity	10	7.809	<0.001	10	6.732	<0.001	10	3.974	<0.001
Time×UVR	5	284.380	<0.001	5	7.734	<0.001	5	27.496	<0.001
Time×lincomycin	5	1 336.637	<0.001	5	40.850	<0.001	5	182.394	<0.001
Time×salinity×UVR	10	9.316	<0.001	10	0.259	0. 989	10	1.432	0.169
Time×salinity×lincomycin	10	24.167	<0.001	10	0.944	0.495	10	5.819	<0.001
Time×UVR×lincomycin	5	67.281	<0.001	5	2.412	0.039	5	6.456	<0.001
Time×salinity×UVR×lincomycin	10	8.857	<0.001	10	1.561	0.125	10	1.026	0.424

The symbol × denotes a synergistic effect; df: degree of freedom; *F*: *F* statistic value; Sig.: *P*-value.

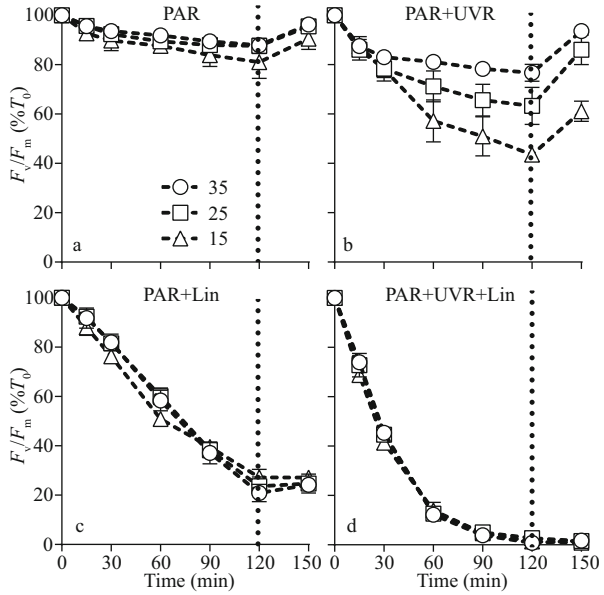

Fig.1 PSII maximum photochemical yield (F_v/F_m) versus high light duration in *Skeletonema costatum* cultures without (a, b) or with (c, d) lincomycin

Cells were exposed to PAR (140 W/m^2) or PAR+UVR (140 W/m^2+ 26 W/m^2) for 120 min, and then shifted to 100 μmol/(m^2·s) of PAR for 30 min. The dotted line indicates the division between high light exposure and recovery period. Data are expressed as the means±SE (*n*=4).

3 RESULT

The maximal photochemical efficiency (F_v/F_m) diminished with increasing bright light exposure in *S. costatum* cells cultured in all salinity (Fig.1 and Table 1). Cells receiving PAR+UVR showed a significant reduction in F_v/F_m (F=439.953, P<0.001), as opposed to those receiving PAR: post bright light exposure, PAR+UVR inhibited F_v/F_m by 56.5% at 15, 36.7% at 25, and 23.4% at 35 (Fig.1b). The addition of lincomycin prompted a significant decline in F_v/F_m (F=1 336.637, P<0.001) in bright light exposed cells, regardless of salinity, especially under UVR exposure (Fig.1d). In the absence of lincomycin, however, F_v/F_m increased to 90.6%–96.3% of the original value when cells were shifted to growth light for 30 min (Fig.1a–b). As expected, cells exposed to lincomycin displayed zero recovery when placed under growth light (Fig.1c–d).

Salinity strongly regulated PsbA synthesis in the *S. costatum* cells: PsbA content decreased in low salinity. Before the high light treatment, the initial PsbA content was 37.81±7.23, 51.02±7.16, and 68.01±5.35 fmol μg/protein at 15, 25, and 35 salinity respectively (F=20.864, P=0.000). Under bright light, however, the level of PsbA in cells with undergoing PSII repair progressively decreased (Fig.2a–b; Table 1). Therefore, light duration, combined with UVR heavily influenced PsbA levels in *S. costatum* cells (F=7.734, P<0.001; Table 1): a 120-min bright light duration, in combination with UVR, decreased PsbA levels by 43.7% at 15, 36.9% at 25, and 29.1% at 35 (F=13.941, P<0.001; F=16.731, P<0.001; Fig.2b; Table 2). A further decrease in PsbA was observed in cells incubated with lincomycin during bright light exposure, irrespective of salinity treatment (F=40.850, P<0.001; Fig.2c–d). Post 30-min recovery under growth light, the PsbA levels in the PAR-exposed cells slight increased to 83.2%–87.4% of the original value (Fig.2a). However, no recovery was observed in cells treated with lincomycin (Fig.2c–d).

To explore the role of salinity and UVR in regulating electron transport on the acceptor region of the PSII protein, alterations in the possibility of electron transfer beyond Q_A (ψ_0) were measured (Fig.3a). Cells cultured in the three salinities conditions produced no significant alterations in ψ_0; however, ψ_0 in cells decreased significantly in response to bright light; the difference between PAR

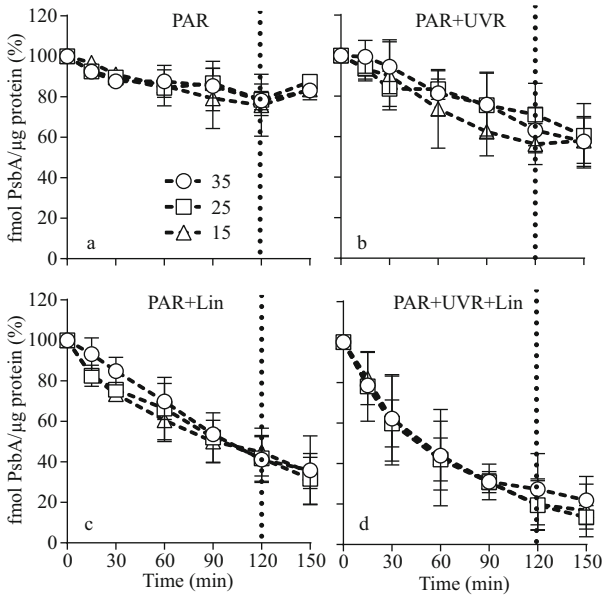

Fig.2 PsbA protein content changes in *S. costatum* cultures treated without (a and b) or with (c and d) lincomycin

Cells were exposed to PAR (140 W/m^2) or PAR+UVR (140 W/m^2+ 26 W/m^2) for 120 min, and then shifted to 100 μmol/(m^2·s) of PAR for 30 min. The dotted line indicates the division between high light exposure and recovery period. The initial PsbA content was 37.81±7.23, 51.02±7.16, and 68.01±5.35 fmol/μg protein for cells grown at 15, 25, and 35 salinity respectively. Data are expressed as the means±SE (n=4).

and PAR+UVR exposed cells at 15 salinity was highly significant (P=0.000; Fig.3a). V_J increased in both PAR and PAR+UVR exposed cells, regardless of salinity changes, especially in cells cultured at 15 exposed to UVR (Fig.3b). The efficiency of conversion within the energy of excitation was determined by measuring the ABS (of antenna chlorophylls) per RC (ABS/RC), the dissipated energy flux per RC (DI_0/RC), the TR (resulting in Q_A reduction) per RC (TR_0/RC), and the ET (further than Q_A^-) per RC (ET_0/RC). The ABS/RC (P=0.000) and DI_0/RC (P=0.000) only increased significantly under UV treatment at 15 salinity (Fig.3c–d). An increase in TR_0/RC was observed in cells receiving high PAR and UVR exposure, particularly in low to medium salinity cultured cells under UVR exposure (Fig.3e). Compared to the original value, only ET_0/RC (P=0.01) significantly decreased in UVR-exposed cells grown in 15 salinity; however, no marked changes occurred between PAR and PAR+UVR exposed cells cultured in all salinity levels (Fig.3f).

The light duration heavily influenced NPQs, and worked in cohort with salinity, UVR, and lincomycin (P<0.001; Fig.4; Table 1): NPQs increased following treatment with bright light, UVR, and lincomycin. This was associated with significant decreases in F_v/F_m (Fig.1) and a loss of the PsbA protein (Fig.2). Low salinity (15), in combination with UVR and lincomycin, decreased NPQs (Fig.4d), and salinity worked in concert with lincomycin to regulate the level of NPQs (P<0.001; Table 3). In the 30-min recovery phase under growth light, NPQs reduced to almost zero in cells cultured at 35 (Fig.4a–b), but maintained high values in cells with lincomycin (Fig. 4c–d).

To identify potential interrelations amongst thermal dissipation, photoinactivation, and clearance of PsbA, the correlation between NPQs induction and K_{pi}/K_{PsbA} was analyzed in all aforementioned growth conditions (Fig.5). Unlike the PAR treatment, diatoms under the PAR+UVR treatment, especially at 25 and 35 salinity, produced elevated NPQs with greater K_{pi} to K_{PsbA} ratio (Fig.5a). Figure 5b shows the plot of K_{PsbA} versus K_{pi}, for lincomycin-exposed cells wherein photoinhibited PSII repair was effectively prevented. Although UVR exposure greatly improved K_{PsbA}, it still lagged behind K_{pi}. All salinity conditions displayed no change in K_{PsbA} (P=0.998) or K_{pi} (P=0.445). The plot of K_{rec} versus K_{PsbA} (Fig.5c) demonstrated that the functional recovery of PSII far surpassed K_{PsbA}. K_{rec} was highest at 35 and decreased significantly with decreasing salinity (P=0.000). UVR treatment significantly reduced K_{rec}, the PAR+UVR induced degradation of PsbA did not measure up to the apparent K_{rec} (Fig.5b–c).

Furthermore, upon transfer to bright light, the CAT activity in *S. costatum* did not change significantly at 25 and 35 salinity, while the presence of UVR significantly increased CAT activity at 15 (P=0.000; Fig.6a). There existed no noticeable influence of salinity concentration or UV treatment on SOD activity (Fig.6b; Table 4).

4 DISCUSSION

When *S. costatum* cells grown at different salinities went from growth light to high light, the maximum PSII quantum yield (F_v/F_m) diminished with exposure time, suggesting a highly suppressive consequence of high PAR and PAR+UVR treatment on photosynthesis, particularly for UVR exposure. It has been extensively demonstrated that photosynthetic organisms are highly susceptible to UVR damage, even with very low dose of UVR (Gao et al., 2009; Li et al., 2015; Williamson et al., 2019). In recent years, the combination effects of UVR and other environmental

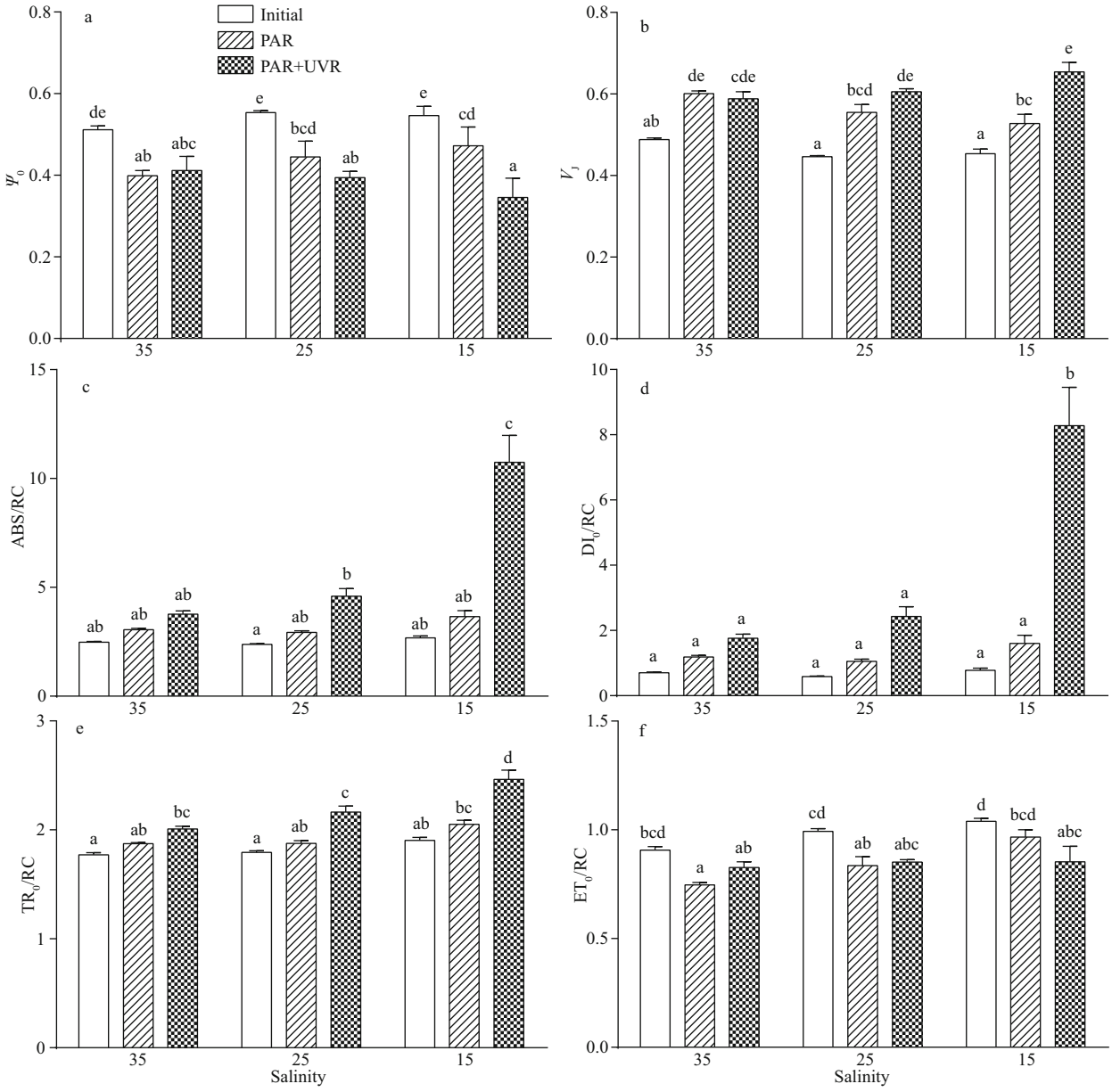

Fig.3 Salinity impact on each parameter in cells of *S. costatum* grown at 15, 25, and 35 salinity before (initial) and after 120-min exposure to PAR or PAR+UVR

a. probability of the transport of an electron beyond Q_A (Ψ_0); b. the relative variable fluorescence at steps J (V_J); c. the electron flow per reaction center (ABS/RC); d. the dissipation flow per reaction center (DI_0/RC); e. the trapping flux per reaction center (TR_0/RC); f. the electron transport flux per reaction center (ET_0/RC). Data are expressed in the means±SE (n=4). Different letters above the error bars indicate significant differences between treatments (P<0.05).

factors have been received much more consideration (Häder et al., 2015). Higher temperatures was reported to mitigate the inhibitory effects of UVR (Halac et al., 2010; Helbling et al., 2011), while increased CO_2 and high salinity could exacerbate the stress of UVR on photosynthetic performance in diatoms (Wu et al., 2017; Gao et al., 2018). In this study, we showed that PSII activity in *S. costatum* was significantly reduced during PAR+UVR exposure and accelerated in cells cultured in low salinity. This may be due to UVR-induced degradation of PsbA and the suppression of new PsbA protein synthesis caused by low salinity. Turnover of the PsbA is essential for PSII repair and activity restoration after photoinactivation (Edelman and Mattoo, 2008; Komenda et al., 2012). When lincomycin—an inhibitor for chloroplast protein synthesis—was added, a significant decrease was observed in both F_v/F_m and in the level of PsbA, indicating the importance of PsbA generation in repair and preservation of active PSII. In the present study,

Table 2 Multivariate analysis of variance measuring the consequences of salinity, UVR, and lincomycin on F_v/F_m and PsbA levels at varying time intervals

Item	F_v/F_m						PsbA					
	120 min			150 min			120 min			150 min		
	df	*F*	Sig.	df	*F*	Sig.	df	*F*	Sig.	df	*F*	Sig.
Salinity	2	18.398	<0.001	2	38.174	<0.001	2	16.731	<0.001	2	17.091	<0.001
UVR	1	439.953	<0.001	1	470.738	<0.001	1	13.941	0.001	1	24.802	<0.001
Lincomycin	1	3 002.268	<0.001	1	7 235.626	<0.001	1	89.645	<0.001	1	148.588	<0.001
Salinity× UVR	2	16.307	<0.001	2	26.471	<0.001	2	0.170	0.844	2	0.920	0.409
Salinity×lincomycin	2	40.649	<0.001	2	52.583	<0.001	2	1.486	0.242	2	2.267	0.120
UVR×lincomycin	1	1.271	0.267	1	32.098	<0.001	1	0.385	0.539	1	1.057	0.312
Salinity×UVR×lincomycin	2	8.290	0.001	2	17.038	<0.001	2	0.287	0.752	2	0.729	0.490

The symbol × denotes a synergistic effect; df: degree of freedom; *F*: *F* statistic value; Sig.: *P*-value.

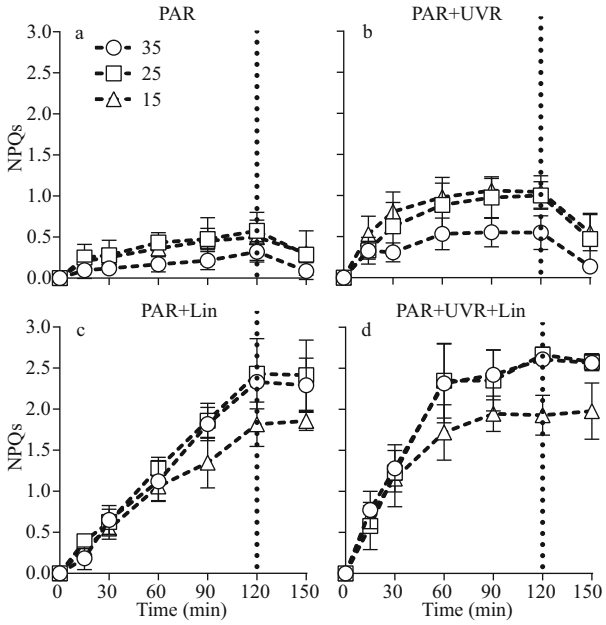

Fig.4 Sustained NPQ (NPQs) responses versus exposure time of high light in *S. costatum* cultures treated without (a, b) or with (c, d) lincomycin

Cells were exposed to PAR (140 W/m²) or PAR+UVR (140 W/m²+ 26 W/m²) for 120 min, and then shifted to 100 μmol/(m²·s) of PAR for 30 min. The dotted line indicates the division between high light exposure and recovery period. Data are expressed as the means±SE (n=4).

salinity, had no effect on PsbA removal rate (K_{PsbA}), whereas UVR accelerated it. The UVR-induced degradation of PsbA was also demonstrated in the diatom *Thalassiosira weissflogii* (Gao et al., 2018). For the effective repair of PsbA following photodamage, the damaged PsbA protein from the thylakoid membrane must be replaced with a newly formed intact protein (Komenda et al., 2012; Eaton-Rye and Sobotka, 2017). In our study, the PSII reaction center complex assembly remained faulty in low salinity conditions as it lacked the newly synthesized PsbA protein for reinsertion. Therefore, although UVR increased PsbA removal, the PSII photochemical activity was likely not restored in low salinity, as shown in Fig.1. UVR-stimulated K_{PsbA} failed to counter the photoinactivation of PSII (K_{pi}), thereby, producing a large quantity of inactivated PSII in UVR-exposed cells.

Multiple studies have demonstrated that UVR promotes the functional loss of Q_A and Q_B quinone electron acceptors and causes damage to the donor regions (Vass et al., 1999; Jiang and Qiu, 2005). In this study, the possibility of the electron transfers beyond Q_A (Ψ_0) reduced significantly upon exposure to high PAR and PAR+UVR, particularly in cells cultured at 15. This indicates that high PAR, in the presence of UVR, damages the acceptor region of the PSII protein in *S. costatum*. Low salinity exacerbates the damaging effect of UVR. However, salinity alone, in the range of 15 to 35, did not regulate PSII acceptor region. Similarly, a significant increase of V_J in cells cultured in 15 under UVR exposure indicated elevated closed PSII reaction centers levels, and consequently, in the level of reduced Q_A at phase J. TR_0/RC is an estimation of electron flow only from the PSII donor region to Q_A, and the expression of TR_0/RC refers only to active PSII reaction centers. Our results indicate that UVR inactivated some PSII reaction centers, and low salinity decreased the PsbA levels. As a result, the dysregulation of the small pool of PSII reaction centers promoted an increase in TR_0/RC, ABS/RC, and DI_0/RC. The ET_0/RC only decreased significantly under UVR exposure in low salinity, with changes in Ψ_0 (Fig.3). Hence, the *S. costatum*

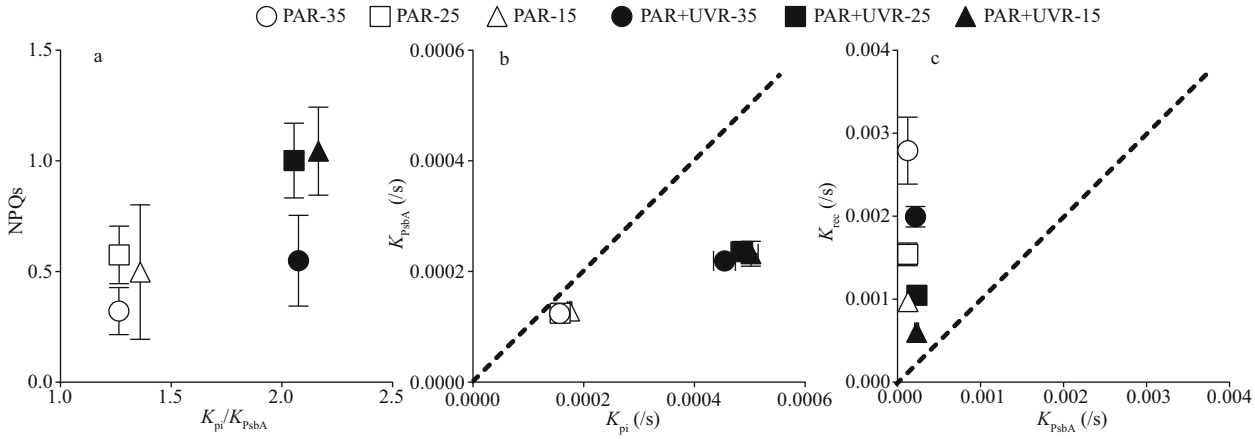

Fig.5 The interrelationship among NPQs, photoinactivation, and PsbA loss in *S. costatum* cultures exposed to PAR or PAR+UVR at varying salinity

a. NPQs (120 min) versus the ratio of K_{pi} to K_{PsbA}; b. PsbA elimination rate constant (K_{PsbA}, /s) plotted versus photoinactivation rate constant (K_{pi}, /s); c. correlation of apparent PSII repair rate constant (K_{rec}, /s) and K_{PsbA} (/s) for *S. costatum*. Dotted line represents 1∶1 ratio. Data are expressed as the means±SE (n=4).

Table 3 Multivariate analysis of variance measuring the consequences of salinity, UVR, and lincomycin on NPQs at varying time intervals

Item	120 min			150 min		
	df	*F*	Sig.	df	*F*	Sig.
Salinity	2	10.177	<0.001	2	4.896	0.13
UVR	1	22.311	<0.001	1	6.058	0.019
Lincomycin	1	643.631	<0.001	1	782.187	<0.001
Salinity×UVR	2	0.162	0.851	2	0.008	0.992
Salinity×lincomycin	2	18.559	<0.001	2	12.480	<0.001
UVR×lincomycin	1	2.235	0.144	1	0.039	0.844
Salinity×UVR×lincomycin	2	1.159	0.326	2	0.512	0.604

The symbol × denotes a synergistic effect; df: degree of freedom; *F*: *F* statistic value; sig.: *P*-value.

Table 4 Multivariate analysis of variance measuring the consequences of salinity and UVR on CAT and SOD activity after 120-min exposure

Item	CAT			SOD		
	F	Sig.	df	*F*	Sig.	df
Salinity	82.944	<0.001	2	2.886	0.095	2
UVR	211.649	<0.001	1	1.292	0.278	1
Salinity×UVR	57.139	<0.001	2	0.425	0.663	2

The symbol × denotes a synergistic effect; df: degree of freedom; *F*: *F* statistic value; Sig.: *P*-value.

cells were unable to maintain PSII activity owing to the synergistic effect of lower salinity and UVR.

Diatoms activate NPQs once photoinactivation overcomes removal of PsbA protein (Wu et al., 2012). NPQ is an essential photo-rescue pathway that releases excess excitation energy as heat (Goss and Jakob, 2010). This study demonstrated that UVR exposure increased NPQs activity in *S. costatum*; which is consistent with the UVR and NPQ studies done on *T. weissflogii* (Gao et al., 2018) and *Gephyrocapsa oceanica* (Jin et al., 2013). In diatoms, NPQ is regulated via the trans-thylakoid proton gradient and the xanthophyll cycle (Lavaud et al., 2004). UVR can stimulate the de-epoxidation of xanthophylls and NPQ (Goss et al., 1999; Sobrino et al., 2005). Our study demonstrated a two-phased response of *S. costatum* to a light challenge, PSII repair is initially accelerated followed by the activation of NPQs. Cells grown in salinity of 15 exhibited more dependence on NPQs to counter the failure of PSII repair, as opposed to those grown in salinity of 35 (Fig.4). A similar response was discovered in another marine diatom, *Thalassiosira pseudonana*, when exposed to sub- or super-optimal growth temperatures under bright light exposure (Yuan et al., 2018). The NPQs were highest in the presence of lincomycin, suggesting a strong role of NPQs in the maintenance of PSII activity or in suppressing photoinactivation when PSII repair is blocked. It is worth noting that NPQ is mostly related to xanthophyll cycle pigments, which is unlikely to be affected by lincomycin theoretically. Meanwhile, the apparently high NPQs values in the presence of lincomycin may be due to the mixup of sustained NPQ with photoinhibitory damage that was elevated by lincomycin. However, the cells grown in salinity of 15, in the presence of lincomycin and irreparable PSII damage, displayed relatively smaller increase in NPQs, as compared to cells grown in salinity of 35.

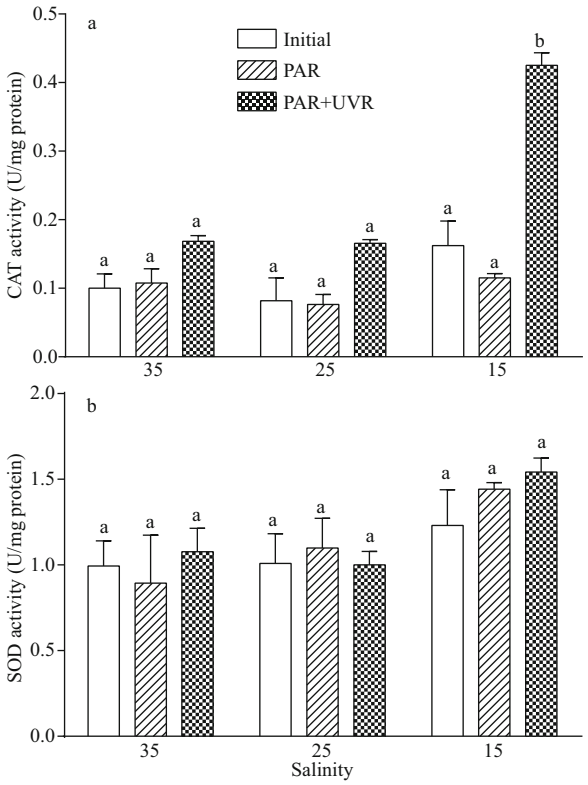

Fig.6 Alterations in CAT (a) and SOD (b) activity in cells of *S. costatum* grown at 15, 25, and 35 salinity before (Initial) and after 120-min exposure to PAR or PAR+UVR

Data are expressed as the means±SE (n=4). Different letters above the error bars indicate significant differences between treatments (P<0.05).

This might be due to the low amount of xanthophylls caused by reduced salinity as those have been found in diatom species *Pseudo-nitzschia australis* (Ayache et al., 2020) and *T. weissflogii* (Bussard et al., 2017). Xanthophylls production is also shown as an antioxidative mechanism deployed to prevent ROS formation (Pelah et al., 2004; Markina and Aizdaicher, 2016). Therefore, although additional studies are required to demonstrate the underlying mechanisms of NPQs induction, we speculated that the xanthophyll reduction in conditions of low salinity might be associated with the dissipation of excess energy, and might contribute to the enhancement of UVR-induced oxidative stress and regulation of the antioxidant defence system (Shiu and Lee, 2005), as evidenced by the significant increase in CAT activity in cells cultured in 15 salinity when exposed to UVR.

5 CONCLUSION

This study was the first to demonstrate the cooperative interaction of UVR and low salinity on PSII function in the marine diatom *S. costatum*. Low salinity reduced PsbA synthesis and worked synergistically with UVR to modify the photochemistry of PSII and, thus, intensified the UVR-induced photoinactivation. Although higher CAT activity and NPQs were induced, they were unable to prevent the damaging combined effect of low salinity and UVR. This study suggests that reduced salinity and increased UVR could potentially affect the abundance and distribution of *S. costatum*, and might affect the formation of *S. costatum*-dominated harmful blooms with the accentuation of climate disturbances.

6 DATA AVAILABILITY STATEMENT

The datasets generated and/or analyzed during the current study are available from the corresponding author on reasonable request.

References

Allakhverdiev S I, Sakamoto A, Nishiyama Y, Inaba M, Murata N. 2000. Ionic and osmotic effects of NaCl-induced inactivation of photosystems I and II in *Synechococcus* sp. *Plant Physiology*, **123**(3): 1047-1056, https://doi.org/10.1104/pp.123.3.1047.

Ayache N, Hervé F, Lundholm N, Amzil Z, Caruana A M N. 2020. Acclimation of the marine diatom *Pseudo-nitzschia australis* to different salinity conditions: effects on growth, photosynthetic activity, and domoic acid content. *Journal of Phycology*, **56**(1): 97-109, https://doi.org/10.1111/jpy.12929.

Bachmann K M, Ebbert V, Adams III W W, Verhoeven A S, Logan B A, Demmig-Adams B. 2004. Effects of lincomycin on PSII efficiency, non-photochemical quenching, D1 protein and xanthophyll cycle during photoinhibition and recovery. *Functional Plant Biology*, **31**(8): 803-813, https://doi.org/10.1071/FP04022.

Bais A F, Bernhard G, McKenzie R L, Aucamp P J, Young P J, Ilyas M, Jöckel P, Deushi M. 2019. Ozone-climate interactions and effects on solar ultraviolet radiation. *Photochemical & Photobiological Sciences*, **18**(3): 602-640, https://doi.org/10.1039/C8PP90059K.

Balzano S, Sarno D, Kooistra W H C F. 2011. Effects of salinity on the growth rate and morphology of ten *Skeletonema* strains. *Journal of Plankton Research*, **33**(6): 937-945, https://doi.org/10.1093/plankt/fbq150.

Barnett A, Méléder V, Blommaert L, Lepetit B, Gaudin P, Vyverman W, Sabbe K, Dupuy C, Lavaud J. 2015. Growth form defines physiological photoprotective capacity in intertidal benthic diatoms. *The ISME Journal*, **9**(1): 32-45, https://doi.org/10.1038/ismej.2014.105.

Bintanja R, Van Oldenborgh G J, Drijfhout S S, Wouters B, Katsman C A. 2013. Important role for ocean warming

and increased ice-shelf melt in Antarctic sea-ice expansion. *Nature Geoscience*, **6**(5): 376-379, https://doi.org/10.1038/ngeo1767.

Blindheim J, Borovkov V, Hansen B, Malmberg S A, Turrell W R, Østerhus S. 2000. Upper layer cooling and freshening in the Norwegian Sea in relation to atmospheric forcing. *Deep Sea Research Part I*: *Oceanographic Research Papers*, **47**(4): 655-680, https://doi.org/10.1016/S0967-0637(99)00070-9.

Boller A J, Thomas P J, Cavanaugh C M, Scott K M. 2015. Isotopic discrimination and kinetic parameters of RubisCO from the marine bloom-forming diatom, *Skeletonema costatum*. *Geobiology*, **13**(1): 33-43, https://doi.org/10.1111/gbi.12112.

Brown C M, MacKinnon J D, Cockshutt A M, Villareal T A, Campbell D A. 2008. Flux capacities and acclimation costs in *Trichodesmium* from the Gulf of Mexico. *Marine Biology*, **154**(3): 413-422, https://doi.org/10.1007/s00227-008-0933-z.

Bussard A, Corre E, Hubas C, Duvernois-Berthet E, Corguillé G L, Jourdren L, Coulpier F, Claquin P, Lopez P J. 2017. Physiological adjustments and transcriptome reprogramming are involved in the acclimation to salinity gradients in diatoms. *Environmental Microbiology*, **19**: 909-925, http://doi: 10.1111/1462-2920.13398.

Campbell D A, Tyystjärvi E. 2012. Parameterization of photosystem II photoinactivation and repair. *Biochimica et Biophysica Acta* (*BBA*)-*Bioenergetics*, **1817**(1): 258-265, https://doi.org/10.1016/j.bbabio.2011.04.010.

Eaton-Rye J J, Sobotka R. 2017. Editorial: assembly of the photosystem II membrane-protein complex of oxygenic photosynthesis. *Frontiers in Plant Science*, **8**: 884, https://doi.org/10.3389/fpls.2017.00884.

Edelman M, Mattoo A K. 2008. D1-protein dynamics in photosystem II: the lingering enigma. *Photosynthesis Research*, **98**(1): 609-620, https://doi.org/10.1007/s11120-008-9342-x.

Falkowski P. 2012. Ocean science: the power of plankton. *Nature*, **483**(7387): S17-S20, https://doi.org/10.1038/483S17a.

Gao G, Gao K S, Giordano M. 2009. Responses to solar UV radiation of the diatom *Skeletonema costatum* (Bacillariophyceae) grown at different Zn^{2+} concentrations. *Journal of Phycology*, **45**(1): 119-129, https://doi.org/10.1111/j.1529-8817.2008.00616.x.

Gao G, Qu L M, Xu T P, Burgess J G, Li X S, Xu J T. 2019. Future CO_2-induced ocean acidification enhances resilience of a green tide alga to low-salinity stress. *ICES Journal of Marine Science*, **76**(7): 2437-2445, https://doi.org/10.1093/icesjms/fsz135.

Gao G, Shi Q, Xu Z G, Xu J T, Campbell D A, Wu H Y. 2018. Global warming interacts with ocean acidification to alter PSII function and protection in the diatom *Thalassiosira weissflogii*. *Environmental and Experimental Botany*, **147**: 95-103, https://doi.org/10.1016/j.envexpbot.2017.11.014.

Gattuso J P, Magnan A, Billé R, Cheung W W L, Howes E L, Joos F, Allemand D, Bopp L, Cooley S R, Eakin C M, Hoegh-Guldberg O, Kelly R P, Pörtner H O, Rogers A D, Baxter J M, Laffoley D, Osborn D, Rankovic A, Rochette J, Sumaila U R, Treyer S, Turley C. 2015. Contrasting futures for ocean and society from different anthropogenic CO_2 emissions scenarios. *Science*, **349**(6243): aac4722, https://doi.org/10.1126/science.aac4722.

Goss R, Jakob T. 2010. Regulation and function of xanthophyll cycle-dependent photoprotection in algae. *Photosynthesis Research*, **106**(1): 103-122, https://doi.org/10.1007/s11120-010-9536-x.

Goss R, Mewes H, Wilhelm C. 1999. Stimulation of the diadinoxanthin cycle by UV-B radiation in the diatom *Phaeodactylum tricornutum*. *Photosynthesis Research*, **59**(1): 73-80, https://doi.org/10.1023/A:1006169901482.

Guillard R R L, Ryther J H. 1962. Studies of marine planktonic diatoms: I. *Cyclotella nana* Hustedt, and *Detonula confervacea* (Cleve) Gran. *Canadian Journal of Microbiology*, **8**(2): 229-239, https://doi.org/10.1139/m62-029.

Häder D P, Gao K S. 2017. The impacts of climate change on marine phytoplankton. *In*: Phillips B F, Pérez-Ramírez M eds. Climate Change Impacts on Fisheries and Aquaculture: A Global Analysis, I. John Wiley & Sons Ltd, Hoboken. p.897-924.

Häder D P, Kumar H D, Smith R C, Worrest R C. 2007. Effects of solar UV radiation on aquatic ecosystems and interactions with climate change. *Photochemical & Photobiological Sciences*, **6**(3): 267-285, https://doi.org/10.1039/B700020K.

Häder D P, Williamson C E, Wängberg S Å, Rautio M, Rose K C, Gao K S, Helbling E W, Sinha R P, Worrest R. 2015. Effects of UV radiation on aquatic ecosystems and interactions with other environmental factors. *Photochemical & Photobiological Sciences*, **14**(1): 108-126, https://doi.org/10.1039/C4PP90035A.

Halac S R, Villafañe V E, Helbling E W. 2010. Temperature benefits the photosynthetic performance of the diatoms *Chaetoceros gracilis* and *Thalassiosira weissflogii* when exposed to UVR. *Journal of Photochemistry and Photobiology B*: *Biology*, **101**(3): 196-205, https://doi.org/10.1016/j.jphotobiol.2010.07.003.

Harrison J W, Smith R E H. 2009. Effects of ultraviolet radiation on the productivity and composition of freshwater phytoplankton communities. *Photochemical & Photobiological Sciences*, **8**(9): 1218-1232, https://doi.org/10.1039/b902604e.

Helbling E W, Buma A G J, Boelen P, Van Der Strate H J, Giordanino M V F, Villafañe V E. 2011. Increase in Rubisco activity and gene expression due to elevated temperature partially counteracts ultraviolet radiation-induced photoinhibition in the marine diatom *Thalassiosira weissflogii*. *Limnology and Oceanography*, **56**(4): 1330-1342, https://doi.org/10.4319/lo.2011.56.4.1330.

Intergovernmental Panel on Climate Change. 2013. The physical science basis. *In*: Stocker T F, Qin D, Plattner G K, Tignor M M B, Allen S K, Boschung J, Nauels A, Xia

Y, Bex V, Midgley P M eds. Climate change 2013: Working Group I Contribution to the Fifth Assessment Report of the Intergovernmental Panel on Climate Change. Cambridge University Press, Cambridge. p.6-10.

Jiang H B, Qiu B S. 2005. Photosynthetic adaptation of a bloom-forming cyanobacterium *Microcystis aeruginosa* (Cyanophyceae) to prolonged UV-B exposure. *Journal of Phycology*, **41**(5): 983-992, https://doi.org/10.1111/j.1529-8817.2005.00126.x.

Jin P, Gao K S, Villafañe V E, Campbell D A, Helbling E W. 2013. Ocean acidification alters the photosynthetic responses of a coccolithophorid to fluctuating ultraviolet and visible radiation. *Plant Physiology*, **162**(4): 2084-2094, https://doi.org/10.1104/pp.113.219543.

Kamenos N A, Hoey T B, Nienow P, Fallick A E, Claverie T. 2012. Reconstructing Greenland ice sheet runoff using coralline algae. *Geology*, **40**: 1095-1098, https://doi.org/10.1130/G33405.1.

Kang E J, Kim J H, Kim K, Kim K Y. 2016. Adaptations of a green tide forming *Ulva linza* (Ulvophyceae, Chlorophyta) to selected salinity and nutrients conditions mimicking representative environments in the Yellow Sea. *Phycologia*, **55**(2): 210-218, https://doi.org/10.2216/15-67.1.

Kirrolia A, Bishnoi N R, Singh N. 2011. Salinity as a factor affecting the physiological and biochemical traits of *Scenedesmus quadricauda*. *Journal of Algal Biomass Utilization*, **2**(4): 28-34.

Kok B. 1956. On the inhibition of photosynthesis by intense light. *Biochimica et Biophysica Acta*, **21**(2): 234-244, https://doi.org/10.1016/0006-3002(56)90003-8.

Komenda J, Sobotka R, Nixon P J. 2012. Assembling and maintaining the Photosystem II complex in chloroplasts and cyanobacteria. *Current Opinion in Plant Biology*, **15**(3): 245-251, https://doi.org/10.1016/j.pbi.2012.01.017.

Kooistra W H C F, Sarno D, Balzano S, Gu H F, Andersen R A, Zingone A. 2008. Global diversity and biogeography of *Skeletonema* species (Bacillariophyta). *Protist*, **159**(2): 177-193, https://doi.org/10.1016/j.protis.2007.09.004.

Lavaud J, Goss R. 2014. The peculiar features of non-photochemical fluorescence quenching in diatoms and brown algae. *In*: Demmig-Adams B, Garab G, Adams III W, Govindjee eds. Non-Photochemical Quenching and Energy Dissipation in Plants, Algae and Cyanobacteria. Springer, Dordrecht. p.421-443.

Lavaud J, Lepetit B. 2013. An explanation for the inter-species variability of the photoprotective non-photochemical chlorophyll fluorescence quenching in diatoms. *Biochimica et Biophysica Acta* (*BBA*)-*Bioenergetics*, **1827**(3): 294-302, https://doi.org/10.1016/j.bbabio.2012.11.012.

Lavaud J, Rousseau B, Etienne A L. 2004. General features of photoprotection by energy dissipation in planktonic diatoms (Bacillariophyceae). *Journal of Phycology*, **40**: 130-137, https://doi.org/10.1046/j.1529-8817.2004.03026.x.

Li W, Gao K, Beardall J. 2015. Nitrate limitation and ocean acidification interact with UV-B to reduce photosynthetic performance in the diatom *Phaeodactylum tricornutum*. *Biogeosciences*, **12**(8): 2383-2393, https://doi.org/10.5194/bg-12-2383-2015.

MacIntyre H L, Kana T M, Geider R J. 2000. The effect of water motion on short-term rates of photosynthesis by marine phytoplankton. *Trends in Plant Science*, **5**(1): 12-17, https://doi.org/10.1016/S1360-1385(99)01504-6.

Markina Z V, Aizdaicher N A. 2016. The effect of lowered salinity of sea water on the growth and photosynthetic pigment content in three strains of the microalgae *Pseudo-nitzschia pungens* (Grunow ex. P.T. Cleve) Hasle, 1993 (Bacillariophyta). *Russian Journal of Marine Biology*, **42**(5): 414-418, https://doi.org/10.1134/S1063074016050060.

Neale P J, Thomas B C. 2017. Inhibition by ultraviolet and photosynthetically available radiation lowers model estimates of depth-integrated picophytoplankton photosynthesis: global predictions for *Prochlorococcus* and *Synechococcus*. *Global Chang Biology*, **23**(1): 293-306, https://doi.org/10.1111/gcb.13356.

Nishiyama Y, Allakhverdiev S I, Murata N. 2006. A new paradigm for the action of reactive oxygen species in the photoinhibition of photosystem II. *Biochimica et Biophysica Acta* (*BBA*)-*Bioenergetics*, **1757**(7): 742-749, https://doi.org/10.1016/j.bbabio.2006.05.013.

Nishiyama Y, Murata N. 2014. Revised scheme for the mechanism of photoinhibition and its application to enhance the abiotic stress tolerance of the photosynthetic machinery. *Applied Microbiology and Biotechnology*, **98**(21): 8777-8796, https://doi.org/10.1007/s00253-014-6020-0.

Nixon P J, Michoux F, Yu J F, Boehm M, Komenda J. 2010. Recent advances in understanding the assembly and repair of photosystem II. *Annals of Botany*, **106**(1): 1-16, https://doi.org/10.1093/aob/mcq059.

Pawlowicz R. 2015. The Absolute Salinity of seawater diluted by riverwater. *Deep Sea Research Part I*: *Oceanographic Research Papers*, **101**: 71-79, https://doi.org/10.1016/j.dsr.2015.03.006.

Pelah D, Sintov A, Cohen E. 2004. The effect of salt stress on the production of canthaxanthin and astaxanthin by *Chlorella zofingiensis* grown under limited light intensity. *World Journal of Microbiology and Biotechnology*, **20**(5): 483-486, https://doi.org/10.1023/B:WIBI.0000040398.93103.21.

Pugkaew W, Meetam M, Yokthongwattana K, Leeratsuwan N, Pokethitiyook P. 2019. Effects of salinity changes on growth, photosynthetic activity, biochemical composition, and lipid productivity of marine microalga *Tetraselmis suecica*. *Journal of Applied Phycology*, **31**(2): 969-979, https://doi.org/10.1007/s10811-018-1619-7.

Radchenko I G, Il'yash L V. 2006. Growth and photosynthetic activity of diatom *Thalassiosira weissflogii* at decreasing salinity. *Biology Bulletin*, **33**(3): 242-247, https://doi.org/10.1134/S106235900603006X.

Rai S V, Rajashekhar M. 2014. Effect of pH, salinity and temperature on the growth of six species of marine phytoplankton. *Journal of Algal Biomass Utilization*,

5(4): 55-59.

Rijstenbil J W. 2005. UV-and salinity-induced oxidative effects in the marine diatom *Cylindrotheca closterium* during simulated emersion. *Marine Biology*, **147**(5): 1063-1073, https://doi.org/10.1007/s00227-005-0015-4.

Rückamp M, Braun M, Suckro S, Blindow N. 2011. Observed glacial changes on the King George Island ice cap, Antarctica, in the last decade. *Global and Planetary Change*, **79**(1-2): 99-109, https://doi.org/10.1016/j.gloplacha.2011.06.009.

Screen J A, Simmonds I. 2010. The central role of diminishing sea ice in recent Arctic temperature amplification. *Nature*, **464**(7293): 1334-1337, https://doi.org/10.1038/nature09051.

Shiu C T, Lee T M. 2005. Ultraviolet-B-induced oxidative stress and responses of the ascorbate-glutathione cycle in a marine macroalga *Ulva fasciata*. *Journal of Experimental Botany*, **56**(421): 2851-2865, https://doi.org/10.1093/jxb/eri277.

Silva P, Thompson E, Bailey S, Kruse O, Mullineaux C W, Robinson C, Mann N H, Nixon P J. 2003. FtsH is involved in the early stages of repair of photosystem II in *Synechocystis* sp PCC 6803. *The Plant Cell*, **15**(9): 2152-2164, https://doi.org/10.1105/tpc.012609.

Sobrino C, Neale P J, Montero O, Lubián L M. 2005. Biological weighting function for xanthophyll de-epoxidation induced by ultraviolet radiation. *Physiologia Plantarum*, **125**(1): 41-51, https://doi.org/10.1111/j.1399-3054.2005.00538.x.

Strasser R J, Srivastava A, Tsimilli-Michael M. 2000. The fluorescence transient as a tool to characterize and screen photosynthetic samples. *In*: Yunus M, Pathre U, Mohanty P eds. Probing Photosynthesis: Mechanism, Regulation & Adaptation. Taylor and Francis, London. p.443-480.

Thorpe L, Andrews T. 2014. The physical drivers of historical and 21st century global precipitation changes. *Environmental Research Letters*, **9**(6): 064024, https://doi.org/10.1088/1748-9326/9/6/064024.

Trenberth K E, Jones P D. 2007. Observations: surface and atmospheric climate change. *In*: Solomon S, Qin D, Manning M, Chen Z, Marquis M, Averyt K B, Tignor M, Miller H L eds. Climate Change 2007: The Physical Science Basis: Contribution of Working Group I to the Fourth Assessment Report of the Intergovernmental Panel on Climate Change. Cambridge University Press, Cambridge. p.235-336.

Tyystjärvi E, Aro E M. 1996. The rate constant of photoinhibition, measured in lincomycin-treated leaves, is directly proportional to light intensity. *Proceedings of the National Academy of Sciences of the United States of America*, **93**(5): 2213-2218, https://doi.org/10.1073/pnas.93.5.2213.

Vartanian M, Desclés J, Quinet M, Douady S, Lopez P J. 2009. Plasticity and robustness of pattern formation in the model diatom *Phaeodactylum tricornutum*. *New Phytologist*, **182**(2): 429-442, https://doi.org/10.1111/j.1469-8137.2009.02769.x.

Vass I, Kirilovsky D, Etienne A L. 1999. UV-B radiation-induced donor-and acceptor-side modifications of photosystem II in the cyanobacterium *Synechocystis* sp. PCC 6803. *Biochemistry*, **38**(39): 12786-12794, https://doi.org/10.1021/bi991094w.

Wang M H, Wang G Z. 2010. Oxidative damage effects in the copepod *Tigriopus japonicus* Mori experimentally exposed to nickel. *Ecotoxicology*, **19**(2): 273-284, https://doi.org/10.1007/s10646-009-0410-6.

Williamson C E, Neale P J, Hylander S, Rose K C, Figueroa F L, Robinson S A, Häder D P, Wängberg S Å, Worrest R C. 2019. The interactive effects of stratospheric ozone depletion, UV radiation, and climate change on aquatic ecosystems. *Photochemical & Photobiological Sciences*, **18**(3): 717-746, https://doi.org/10.1039/C8PP90062K.

Wu H Y, Cockshutt A M, McCarthy A, Campbell D A. 2011. Distinctive photosystem II photoinactivation and protein dynamics in marine diatoms. *Plant Physiology*, **156**(4): 2184-2195, https://doi.org/10.1104/pp.111.178772.

Wu H Y, Roy S, Alami M, Green B R, Campbell D A. 2012. Photosystem II photoinactivation, repair, and protection in marine centric diatoms. *Plant Physiology*, **160**(1): 464-476, https://doi.org/10.1104/pp.112.203067.

Wu Y P, Zhu Y C, Xu J T. 2017. High salinity and UVR synergistically reduce the photosynthetic performance of an intertidal benthic diatom. *Marine Environmental Research*, **130**: 258-263, https://doi.org/10.1016/j.marenvres.2017.08.004.

Xu J K, Sun J Z, Beardall J, Gao K S. 2020. Lower salinity leads to improved physiological performance in the Coccolithophorid *Emiliania huxleyi*, which partly ameliorates the effects of ocean acidification. *Frontiers in Marine Science*, **7**: 704, https://doi.org/10.3389/fmars.2020.00704.

Yan T, Zhou M J, Qian P Y. 2002. Combined effects of temperature, irradiance and salinity on growth of diatom *Skeletonema costatum*. *Chinese Journal of Oceanology and Limnology*, **20**(3): 237-243, https://doi.org/10.1007/BF02848852.

Young J N, Morel F M M. 2015. Biological oceanography: the CO_2 switch in diatoms. *Nature Climate Change*, **5**(8): 722-723, https://doi.org/10.1038/nclimate2691.

Yuan W B, Gao G, Shi Q, Xu Z G, Wu H Y. 2018. Combined effects of ocean acidification and warming on physiological response of the diatom *Thalassiosira pseudonana* to light challenges. *Marine Environmental Research*, **135**: 63-69, https://doi.org/10.1016/j.marenvres.2018.01.016.